Theoretical analysis of carrier heating effect in semiconductor optical amplifiers

Ghafouri-Shiraz, Hooshang; Xia, Mingjun

DOI:
10.1007/s11082-014-0088-8

Theoretical analysis of carrier heating effects in semiconductor optical amplifiers

Mingjun Xia and H. Ghafouri-Shiraz

Abstract Carrier heating effects strongly influence carrier dynamics in semiconductor optical amplifiers (SOAs). Accurate analysis of carrier heating effects is important in establishing complete model of SOAs. This paper reports an accurate and simple analytical method of carrier heating effects in semiconductor optical amplifiers by using the global approximations of Fermi-Dirac integrals of 3/2 order and Fermi-Dirac integrals of 1/2 order. The relation between Fermi-Dirac integral of 3/2 order and Fermi-Dirac integral of 1/2 order is adopted to remove the derivates of Fermi-Dirac integral in the analytical process. The picosecond pulse amplification for input signals having different peak powers is studied with and without carrier heating effects. It is found that carrier heating effects impose a more distortion on the amplified pulse, including suppressing the peak power value and increasing the peak temporal shift of amplified output signal. When the peak power value of input signal is higher or the pump current is larger, the influences from carrier heating are further enhanced.

Keywords Semiconductor optical amplifiers, Carrier heating effects, Nonlinear optics, optical communication

1. Introduction

Carrier heating effects have been researched because of their importance in influencing the high-speed performance of SOAs [1-3].The effects of carrier heating intensify the nonlinear gain, which affects the modulation bandwidth and even leads to the cross talk between multiplexed signals [4-9]. The basic mechanisms responsible for carrier heating effects are carrier injection, non-radiative recombination, free carrier absorption, stimulated emission and spontaneous emission [10]. Accurate calculation of this effect enables us to better analyze the carrier dynamics during the signal amplification process. The SOA dynamic model considering carrier heating effects is complex, which leads to lots of computation time in the dynamic simulation of SOAs. Thus, an accurate and simple analytical method for carrier heating effects is necessary to establish a complete SOA model.

James M. Dailey et. have expressed the carrier energy density using Fermi-Dirac integral of 3/2 order, which is used to calculate the carrier heating effects in SOAs. However, it did not give detailed derivation and analysis. Fermi Dirac integral of 3/2 order and Fermi Dirac integral of 1/2 order have been suggested for carrier density in a semiconductor band and carrier energy density of an electronic gas [11-12], but Fermi-Dirac integral of 3/2 order and 1/2 order can only be evaluated numerically without approximation [13]. If a high-accuracy Fermi-Dirac integral approximation is chosen, the model computation time is longer. Our analysis presents how to combine the global approximation of Fermi Dirac integral 3/2 order and the global approximation of Fermi Dirac integral of 1/2 order to calculate the energy density, and further analyze the carrier heating effects in SOAs.

In this paper, we study the influences from carrier heating on picosecond pulse amplification using the new analytical method. Carrier heating effects in SOAs are described as the carrier temperature changes. Detailed derivation process of carrier heating effects in SOAs is given. The relation between Fermi Dirac integral of 1/2 order and 3/2 order is adopted to remove the derivate of Fermi Dirac integral of 3/2 order. Global approximations of Fermi-Dirac integrals of 3/2 order and 1/2 order are adopted to calculate the carrier temperature change caused by carrier heating effects. Besides, simpler approximations of Fermi-Dirac integral of 1/2 order are suggested based on the different distributions of the conduction band and the valence band. The effects of carrier heating on picosecond pulse amplification are analyzed. The changes of gain coefficient, carrier density and carrier temperature during the picosecond pulse amplification are given with and without carrier heating effects.

This paper is organized as the following. Section II presents the theory of carrier heating effects and gain modelling of SOA. In

Mingjun Xia
School of Electronic, Electrical and Computer Engineering, University of Birmingham
Birmingham, B15 2TT, UK
e-mail:MXX322@bham.ac.uk

H. Ghafouri-Shiraz (Corresponding author)
School of Electronic, Electrical and Computer Engineering, University of Birmingham
Birmingham, B15 2TT, UK
e-mail: ghafourh@bham.ac.uk

Section III, Simulation results of carrier heating effects on picosecond pulse amplification in SOAs are discussed. Conclusions are given in Section IV.

2 Theory

2.1 Carrier heating effects in SOAs

The temperature dynamics in SOAs can be given by the following expression [1], [14]

$$\frac{dT}{dt} = \frac{1}{\partial U/\partial T}\left(\frac{dU}{dt} - \frac{\partial U}{\partial N}\frac{dN}{dt}\right) - \frac{T - T_0}{\tau} \tag{1}$$

Here, T is the carrier temperature, U is the total plasma energy, N is the carrier density, τ is the temperature recovery time and T_0 is the lattice temperature. $\frac{dU}{dt}$ is obtained using the expression of the rate of energy changes due to stimulated emission, spontaneous emission, free carrier and intervalenceband absorptions [14-15].

$$\begin{aligned}\frac{dU}{dt} = &-\upsilon_g \sum_i (h\nu_i - E_g(N))g(N,\nu_i)(S_{\nu_i}^+ + S_{\nu_i}^-) + \\ &\upsilon_g \alpha_{FC} N \sum_i h\nu_i (S_{\nu_i}^+ + S_{\nu_i}^-) - \\ &\upsilon_g \sum_j (h\nu_j - E_g(N))g(N,\nu_j)(E_{\nu_j}^+ + E_{\nu_j}^-) + \\ &\upsilon_g \alpha_{FC} N \sum_j h\nu_j (E_{\nu_j}^+ + E_{\nu_j}^-)\end{aligned} \tag{2}$$

Where, υ_g is the group velocity, h is the Planck constant, ν_i and ν_j denote the frequency of input signal and the frequency of spontaneous emission, respectively, $E_g(N)$ is the bandgap energy, Γ is the optical confinement factor, g is the material gain, α_{FC} is the free carrier absorption coefficient, $S_{\nu_i}^+$ and $S_{\nu i}^-$ are the forward and backward propagation photon densities of input signal, $E_{\nu_j}^+$ and $E_{\nu_j}^-$ are the forward and backward photon densities due to the amplified spontaneous emission (ASE) of the amplifier.

In the above equation, the photon densities are obtained by the propagation rate equations of the incident optical field and spontaneous emission

$$\left(\frac{\partial}{\partial t} \pm \upsilon_g \frac{\partial}{\partial z}\right) S_{\nu_i}^{\pm} = \upsilon_g S_{\nu_i}^{\pm} (\Gamma g(N,\nu_i) - \alpha_0) \tag{3}$$

$$\left(\frac{\partial}{\partial t} \pm \upsilon_g \frac{\partial}{\partial z}\right) E_{\nu_j}^{\pm} = \upsilon_g E_{\nu_j}^{\pm} (\Gamma g(N,\nu_j) - \alpha_0) + R_{sp}(\nu_j, N) \tag{4}$$

Where, α_0 is the waveguide loss, R_{sp} is the spontaneous emission rate, and the expression is given in [14]. Furthermore, $\frac{dN}{dt}$ is obtained by the following travelling wave rate equation for the carrier density.

$$\begin{aligned}\frac{dN}{dt} = &\frac{I}{qV} - \Gamma\upsilon_g \sum_{\nu_i} g(N,\nu_i)(S_{\nu_i}^+ + S_{\nu_i}^-) - \\ &\Gamma\upsilon_g \sum_{\nu_j} g(N,\nu_j)(E_{\nu_j}^+ + E_{\nu_j}^-) - AN - BN^2 - CN^3\end{aligned} \tag{5}$$

Where, I is the injected current, q is the magnitude of a unit charge, V is the active area volume. A, B, and C are linear recombination coefficient, Bi-molecular recombination coefficient and Auger recombination coefficient, respectively.

One key point of calculating the carrier temperature changes due to carrier heating effects is to calculate the two partial differential items $\frac{\partial U}{\partial T}$ and $\frac{\partial U}{\partial N}$. They are evaluated by the following energy density expression [14].

$$U = \frac{2}{\sqrt{\pi}} KT(N_c F_{3/2}^c + N_v F_{3/2}^v) \tag{6}$$

Where, K is the Boltzmann constant, N_c and N_v are the effective density of states in the conduction and valence bands, which can be expressed as [13]

$$N_c = 2(\frac{2\pi m_e^* KT}{h^2})^{3/2} \tag{7}$$

$$N_v = 2(\frac{2\pi m_v^* KT}{h^2})^{3/2} \tag{8}$$

Where,

$$m_v^* = (m_{hh}^{3/2} + m_{lh}^{3/2})^{2/3} \tag{9}$$

m_e^* is the effective mass of electrons in the conduction band, m_{hh} and m_{lh} are the effective mass of a heavy hole and the effective mass of a light hole in the valence band.

In Eq. (6), $F_{3/2}^c$ and $F_{3/2}^v$ are known as the Fermi-Dirac integral of 3/2 order for the conduction band and valence band, respectively. They are given by:

$$F_{3/2}^c = \int_0^{+\infty} \frac{x_c^{3/2}}{\exp(x_c - \varepsilon_c) + 1} dx_c \tag{10}$$

$$F_{3/2}^v = \int_0^{+\infty} \frac{x_v^{3/2}}{\exp(x_v - \varepsilon_v) + 1} dx_v \tag{11}$$

$$\varepsilon_c = (E_{Fc} - E_c) / KT \tag{12}$$

$$\varepsilon_v = (E_v - E_{Fv}) / KT \tag{13}$$

Where, E_{Fc} and E_{Fv} are the quasi-Fermi levels in the conduction and valence bands, E_c and E_v are the conduction band edge and the valence band edge. Then, the two partial differential items can be expressed as

$$\frac{\partial U}{\partial T} = \frac{2}{\sqrt{\pi}} K(N_c F_{3/2}^c + N_v F_{3/2}^v) + \frac{2}{\sqrt{\pi}} KT(\frac{\partial (N_c F_{3/2}^c)}{\partial T} + \frac{\partial (N_v F_{3/2}^v)}{\partial T}) \tag{14}$$

$$\frac{\partial U}{\partial N} = \frac{2}{\sqrt{\pi}} KT(N_c \frac{\partial (F_{3/2}^c)}{\partial N} + N_v \frac{\partial (F_{3/2}^v)}{\partial N}) \tag{15}$$

From Eq. (6)-(13), we know that it is difficult to calculate the two partial differential items without approximation due to the complexity of Fermi Dirac integral. Also, it should be noted the quasi-Fermi levels are functions of both temperature and carrier density, which further increases the computation difficulty.

In the analysis, we rewrite the differential items on the right hand side of Eq. (14) and Eq. (15) as the following equations.

$$\frac{\partial (N_c F_{3/2}^c)}{\partial T} = \frac{\partial N_c}{\partial T} F_{3/2}^c + N_c \frac{\partial F_{3/2}^c}{\partial \varepsilon_c} \frac{\partial \varepsilon_c}{\partial T} \tag{16}$$

$$\frac{\partial (N_v F_{3/2}^v)}{\partial T} = \frac{\partial N_v}{\partial T} F_{3/2}^v + N_v \frac{\partial F_{3/2}^v}{\partial \varepsilon_v} \frac{\partial \varepsilon_v}{\partial T} \tag{17}$$

$$N_c \frac{\partial(F_{3/2}^c)}{\partial N} = N_c \frac{\partial(F_{3/2}^c)}{\partial \varepsilon_c} \frac{\partial \varepsilon_c}{\partial N} \tag{18}$$

$$N_v \frac{\partial(F_{3/2}^v)}{\partial N} = N_v \frac{\partial(F_{3/2}^v)}{\partial \varepsilon_v} \frac{\partial \varepsilon_v}{\partial N} \tag{19}$$

Then, the property between the Fermi-Dirac integral of 3/2 order and the Fermi-Dirac integral of 1/2 order is adopted [16].

$$\frac{dF_{3/2}(\varepsilon)}{d\varepsilon} = \frac{3}{2} F_{1/2}(\varepsilon) \tag{20}$$

Substituting Eq. (12), (13) and (20) into Eq. (16)-(19), we can express the four differential items as

$$\frac{\partial(N_c F_{3/2}^c)}{\partial T} = \frac{\partial N_c}{\partial T} F_{3/2}^c + \frac{3}{2} N_c F_{1/2}^c \times \left(\frac{\frac{KT(\partial E_{Fc})}{\partial T} - K(E_{Fc} - E_c)}{(KT)^2}\right) \tag{21}$$

$$\frac{\partial(N_v F_{3/2}^v)}{\partial T} == \frac{\partial N_v}{\partial T} F_{3/2}^v + \frac{3}{2} N_v F_{1/2}^v \times \left(\frac{-\frac{KT(\partial E_{Fv})}{\partial T} - K(E_v - E_{Fv})}{(KT)^2}\right) \tag{22}$$

$$N_c \frac{\partial(F_{3/2}^c)}{\partial N} = \frac{3}{2} N_c F_{1/2}^c (KT)^{-1} \frac{\partial E_{Fc}}{\partial N} \tag{23}$$

$$N_v \frac{\partial(F_{3/2}^v)}{\partial N} = -\frac{3}{2} N_v F_{1/2}^v (KT)^{-1} \frac{\partial E_{Fv}}{\partial N} \tag{24}$$

In Eq. (21) to Eq. (24), the differential items of Fermi-Dirac integral have been removed, which simplifies the calculation $\frac{\partial U}{\partial T}$ and $\frac{\partial U}{\partial N}$. At the same time, the derivates of quasi-Fermi levels in the conduction and valence bands with respect to temperature and carrier density can be obtained through the numerical calculation based on the following approximation formula [17].

$$E_{Fc} = \left(\ln u_c + \frac{u_c}{[64 + 0.05524 u_c (64 + u_c^{1/2})]^{1/4}}\right) KT \tag{25}$$

$$E_{Fv} = -\left(\ln u_v + \frac{u_v}{[64 + 0.05524 u_v (64 + u_v^{1/2})]^{1/4}}\right) KT \tag{26}$$

Where

$$u_c = \frac{N}{N_c} \qquad u_v = \frac{N}{N_v} \tag{27}$$

Next, an analytical approximation for the Fermi-Dirac integral 3/2 order is chosen. Here, ε is valid in the whole range from $-\infty$ to $+\infty$ with a relative error below 0.7% [16].

$$F_{3/2}(\varepsilon) = \left[\frac{\frac{5}{2} \times 2^{5/2}}{(2.64 + \varepsilon + (|\varepsilon - 2.64|^{9/4} + 14.9)^{4/9})^{5/2}} + \frac{e^{-\varepsilon}}{\Gamma(5/2)}\right]^{-1} \tag{28}$$

Besides, in the process of removing the differential items of the Fermi-Dirac integral of 3/2 order, Fermi-Dirac integral of 1/2 order appears in Eq. (21)-(24). Thus, the following global approximation for Fermi-Dirac integral of 1/2 order [18] is adopted.

$$F_{1/2}(\varepsilon) \approx \frac{1}{2}\sqrt{\pi}\left[\frac{3}{4}\sqrt{\pi} a^{-3/8}(\varepsilon) + \exp(-\varepsilon)\right]^{-1} \tag{29}$$

$$a(\varepsilon) = \varepsilon^4 + 33.6\varepsilon\{1 - 0.68\exp[-0.17(\varepsilon + 1)^2]\} + 50 \tag{30}$$

Where, ε is valid from $-\infty$ to $+\infty$. Substituting the global approximations for Fermi-Dirac integral of 3/2 order and Fermi-Dirac integral of 1/2 order into Eq. (21)-Eq. (24), the two differential items $\frac{\partial U}{\partial T}$ and $\frac{\partial U}{\partial N}$ is calculated. Therefore, the change of the carrier temperature due to carrier heating effects can be obtained by Eq. (1).

The method mentioned above simplifies the calculation process of carrier heating effects for SOAs. It should be noted that the method applies for QW-SOAs only when the discontinuous distribution [19] of the energy density and the coupling effects among the valence bands are ignored. Besides, based on the valid range of ε_c and ε_v, which are related to the quasi-Fermi level and the band edge, simpler non-global approximations for Fermi-Dirac integral of 1/2 order [13] can be adopted to calculate the carrier heating effects in SOAs.

2.2 Gain Modelling of SOAs

The materials of the modelled SOAs are $In_{1-x}Ga_xAs_yP_{1-y}$ lattice matched to InP. y and x are the corresponding molar fractions of As and Ga. The optical gain of the active region is a function of the frequency and carrier density. The material gain coefficient $g(\omega, N)$ is given by [20]

$$g(\omega,N)=\frac{c^2}{2\hbar^{1/2}n_r^2\tau_s\omega^2}\left(\frac{2m_e^*m_{hh}}{\hbar(m_e^*+m_{hh})}\right)^{3/2}\times\sqrt{\hbar\omega-E_g(N)}\,(f_c(\omega)-f_v(\omega)) \tag{31}$$

Where, ω is the optical angular frequency, $\hbar$ is the Planck constant divided by 2π, n_r is the refractive index of the active region material, τ_s is the radiative carrier recombination lifetime, c is the speed of light in free space, $f_c(\omega)$ and $f_v(\omega)$ are the Fermi-Dirac distribution functions in the conduction and valence bands, which can be expressed as[20]-[21]

$$f_c(\omega,N)=1/(1+\exp(\frac{E_a-E_{Fc}}{KT})) \tag{32}$$

$$f_v(\omega,N)=1/(1+\exp(\frac{E_b-E_{Fv}}{KT})) \tag{33}$$

Where,

$$E_a=(\hbar\omega-Eg(N))\frac{m_{hh}}{m_e^*+m_{hh}} \tag{34}$$

$$E_b=-(\hbar\omega-Eg(N))\frac{m_e^*}{m_e^*+m_{hh}} \tag{35}$$

E_{Fc} and E_{Fv} are calculated through Eq.(25) and Eq. (26). The bandgap energy $E_g(N)$ can be expressed as [22]

$$E_g(N)=E_{g0}-qK_gN^{1/3}) \tag{36}$$

Where, K_g is the coefficient of the bandgap shrinkage. Since the lattice of $In_{1-x}Ga_xAs_yP_{1-y}$ is matched to InP, the initial bandgap energy E_{g0} is given by [23]

$$E_{g0}=q(1.35-0.775y+0.149y^2) \tag{37}$$

The carrier recombination lifetime $\tau_s(N)$ is approximated by [22]

$$\tau_s(N)=1/(A+BN) \tag{38}$$

Eq. (31)-Eq. (38) give the gain model of SOAs, which is employed to calculate the propagations of the incident optical filed and the spontaneous emission through Eq. (3) -Eq. (5).

Table 1
Parameters used in the simulation

Symbol	Description	Value
n	Background refractive index	3.22
α_{FC}	Free carrier absorption	$0.5\times10^{-21}m^2$
A	Linear recombination	$1\times10^{7}s^{-1}$
B	Bi-molecular recombination	$5.6\times10^{-16}m^3s^{-1}$
C	Auger recombination	$3\times10^{-41}m^6s^{-1}$
K_g	Bandgap shrinkage coefficient	$0.9\times10^{-10}m$
τ	Temperature recovery time	$1ps$
α_0	Waveguide loss	$12000m^{-1}$
Γ	Confinement factor	0.45
N_0	Transparent carrier density	$1.0\times10^{24}m^{-3}$
I	Input current	$100mA$
W	SOA width	$1\mu m$
D	SOA thickness	$0.4\mu m$
L	SOA length	$750\mu m$
m_e^*	Effective mass of electron in the CB	$4.07\times10^{-32}kg$
m_{hh}	Effective mass of heavy hole in the VB	$4.19\times10^{-31}kg$
m_{lh}	Effective mass of light hole in the VB	$5.01\times10^{-32}kg$

3 Results

In the following, the influences of carrier heating on the picosecond pulse amplification is studied using the above analytical method of carrier heating effects in SOAs and gain modelling of SOAs. In the simulation, the photon density and carrier density are obtained using the step-transition method [24] by solving the travelling wave rate equations (Eq. (3)-Eq. (5)). The amplifier cavity is divided into 200 sections. The unchirped Gaussian pulse input signal is centered at $3ps$, having a wavelength of $1550nm$, FWHM $2ps$, and at first, its peak power value is10mw. Other simulation parameters are given in Table 1.

Fig.1 shows the variation of average gain coefficient in the amplifier cavity with and without carrier heating effects while the variation of average carrier density in the amplifier cavity is shown in Fig. 2. As shown in Fig. 1, the gain coefficient without carrier heating effects is larger than the gain coefficient with carrier heating effects before $2.15ps$. This is because the carrier temperature increase due to carrier heating effects leads to the gain suppression. As the carrier temperature increases, the quasi-Fermi level in the conduction band decreases while the quasi-Fermi level in the valence band increases. After $2.15ps$, the gain coefficient without carrier heating effects is smaller than the gain coefficient with carrier heating effects. This can be explained that, the input signal obtains bigger amplification without the influences of carrier heating in the initial stage, which reduces largely the carrier density. Thus, after $2.15ps$, the gain coefficient without carrier heating effects becomes smaller than that with carrier heating effects due to the low carrier density level, which can be observed in Fig. 2. Fig. 2 shows that when carrier heating effects are considered, the average carrier density level is higher, which will shorten the carrier recovery time.

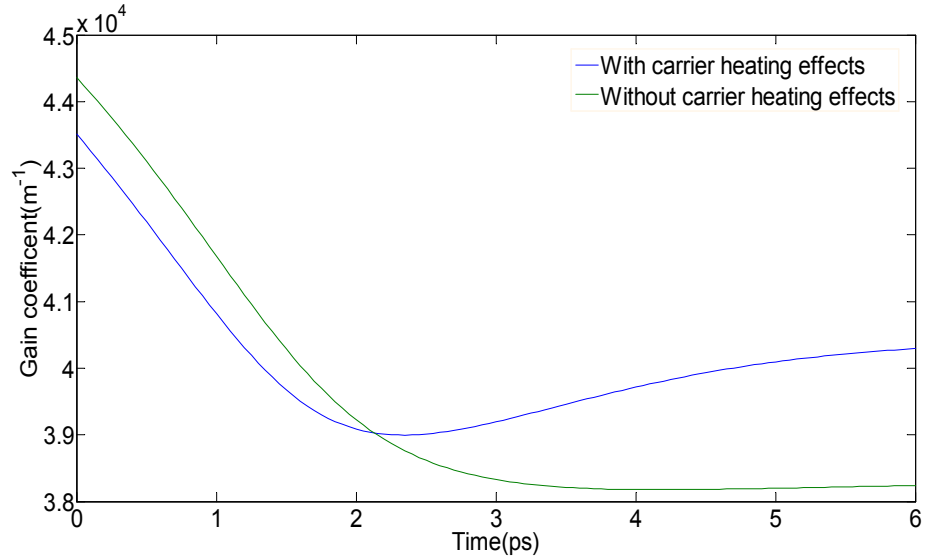

Fig. 1 Variation of the average gain coefficient in SOA with and without carrier heating effects during the pulse amplification process

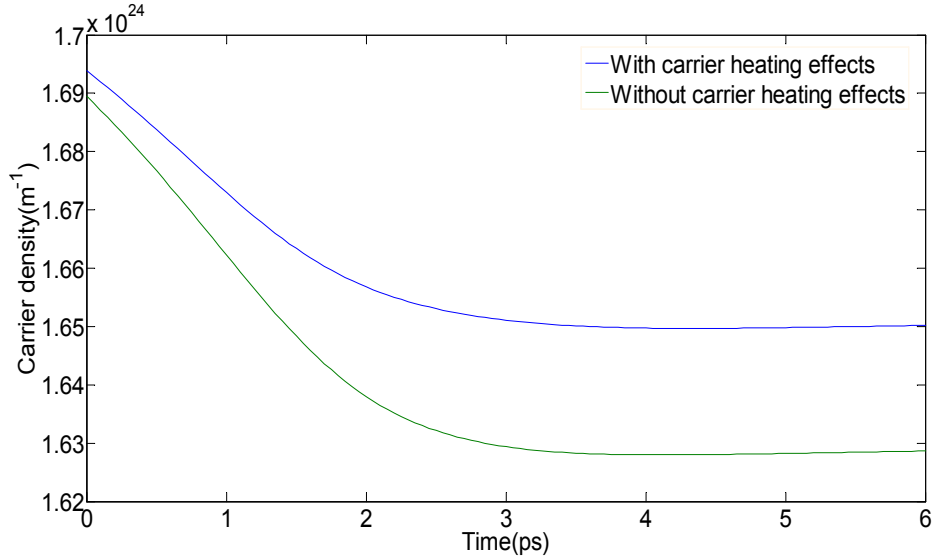

Fig. 2 Variation of the average carrier density in SOA with and without carrier heating effects during the pulse amplification process

Fig. 3 shows the variations of the gain coefficient and the carrier temperature near the exit facet of the amplifier cavity during the pulse amplification process. From this figure, it is observed that the variation of carrier temperature due to carrier heating effects reaches the peak point at $\Delta T = 19.20K$ and then decreases. It is because the photon densities in the SOA increase and then fall as the input signal changes. At the same time, the gain coefficient decreases due to the carrier temperature increase and the carrier density decrease during the pulse amplification process. It should be noted that when the temperature change increases to the largest value, the gain coefficient does not reach the lowest. It is mainly because the carrier density goes on decreasing, which can be known in Fig. 2.

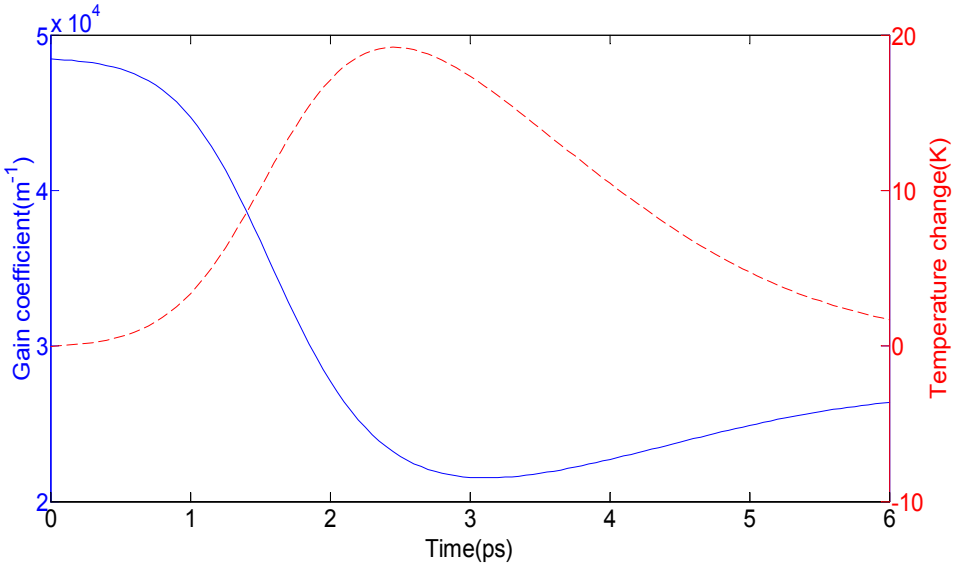

Fig.3 Variations of gain coefficient and carrier temperature near the exit facet of amplifier cavity

Next, the responses of two ideal Gaussian pulses both having the same FWHM of 2ps but different peak values of $10mw$ and $100mw$ both centered at 3ps are shown in Fig. 4 and Fig. 5. When the peak power value of the input pulse is $10mw$ (Fig. 4), carrier heating effects have reduced the peak power values of the output signal from $2.34mw$ to $1.63mw$ and increased its peak temporal shift from $1.05ps$ to $1.2ps$. When the peak power value of the input signal is $100mw$ (Fig. 5), the peak power values of the output signal with and without carrier heating effects are $2.40w$ and $3.78w$, respectively, and In this case, the peak temporal shifts are $2ps$ and $1.85ps$ .We can see that carrier heating effects reduce the peak power value of the amplified output signal and enlarge the peak temporal shift. Comparison of Fig. 4 and Fig. 5 shows that when the peak power value of the input signal is larger, carrier heating effects cause a more significant distortion of the amplified output signal, including lower peak power value of the amplified output signal and larger peak temporal shift of the amplified output signal.

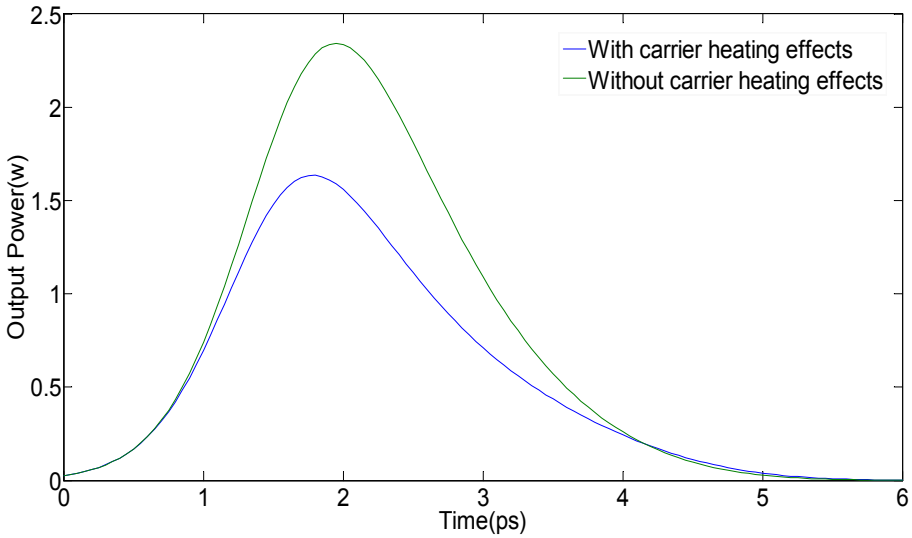

Fig.4 Picosecond pulse amplification of SOA with and without carrier heating effects ($Peak = 10mw$)

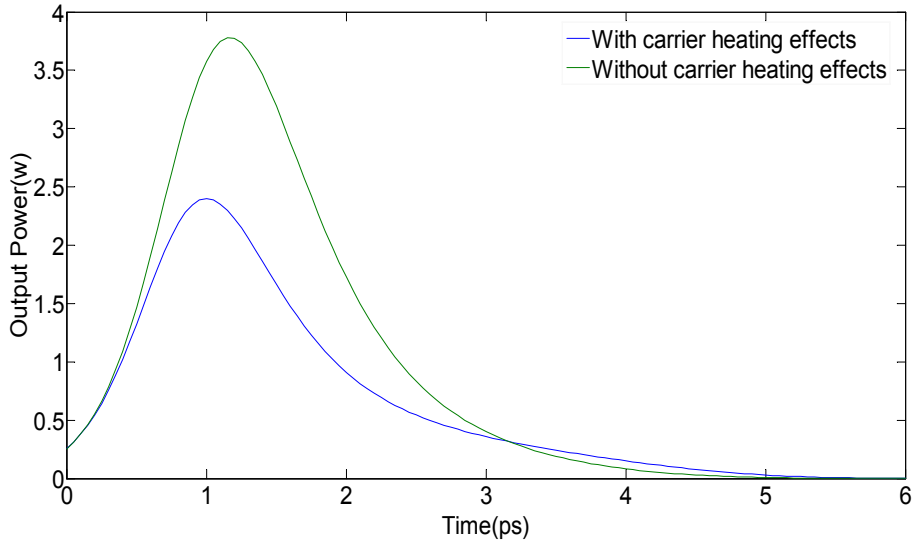

Fig.5 Picosecond pulse amplification of SOA with and without carrier heating effects ($Peak = 100mw$)

Fig.6 shows the variations of carrier temperature near the exit facet of the amplifier cavity when the input signals have different peak power values ($10mw$ and $100mw$). As seen in this figure, the carrier temperature reaches the largest values at $319.20K$ and $324.83K$, respectively. This is because when the peak power value of the input signal is $100mw$, the optical field (stimulated emission) and free carrier absorptions in the amplification cavity are larger, which leads to the bigger changing rate of energy density and carrier density. When the peak power value of the input signal is $100mw$, the peak of the carrier temperature arrives earlier. The reason is that the output signal is earlier saturated when the input peak power is higher.

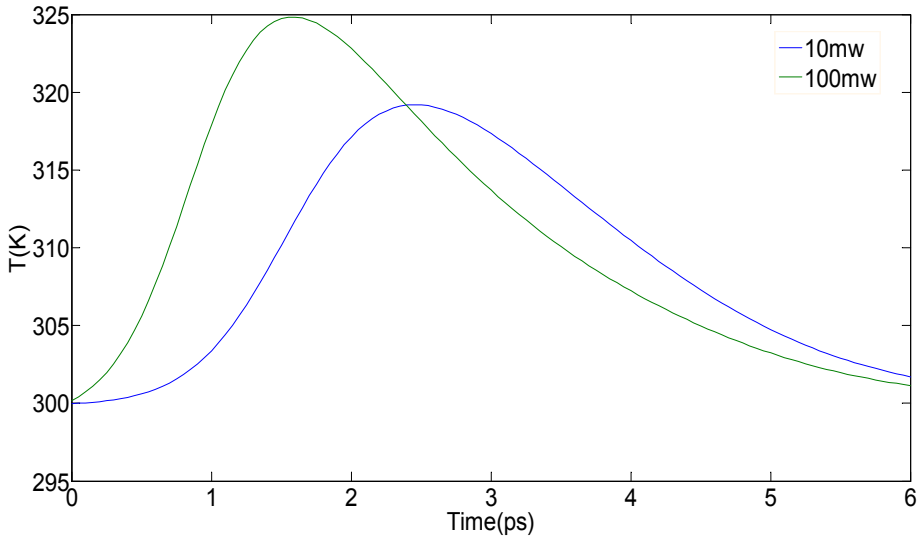

Fig.6 Variation of the carrier temperature near the exit facet of the amplifier cavity during the pulse amplification with different input signals

Fig.7 shows the variations of carrier temperature near the exit facet of the amplifier cavity when different pump currents ($100mA$ and $120mA$) are adopted. The peak power of the input signal is $10mw$ in both cases. Referring to this figure, it is found that when the pump currents are $100mA$ and $120mA$, the peaks of carrier temperature are $319.20K$ and $340.35K$, respectively. As the pump current increases, the temperature change due to carrier heating effects beocmes larger. This is because the increase of the pump current leads to the increase of the carrier density and photon density in the amplifier cavity. Thus, the effects of carrier heating are enhanced.

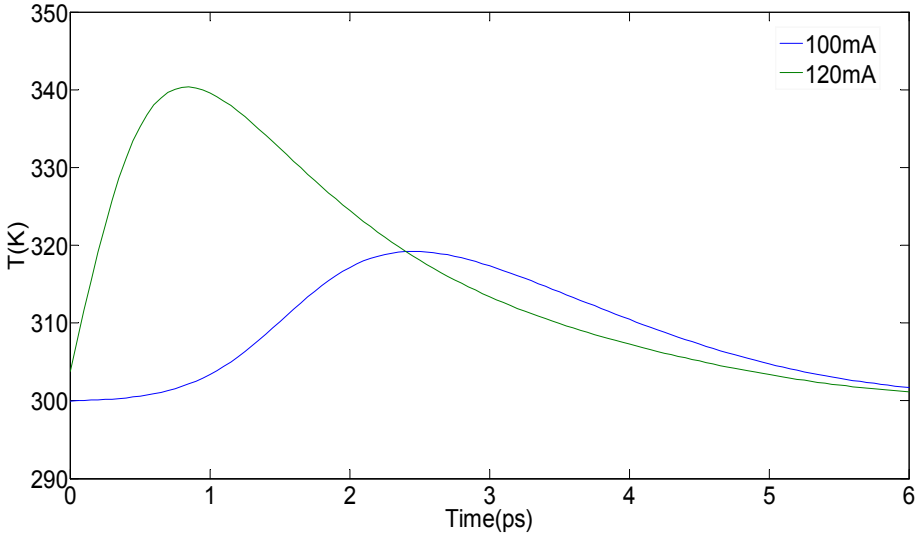

Fig.7 Variation of the carrier temperature near the exit facet of the amplifier cavity during the pulse amplification with different pump currents

4 Conclusions

This paper presents a new analytical method for carrier heating effects in SOAs by using both Fermi-Dirac integral of 3/2 order and Fermi-Dirac integral of 1/2 order. The relation between Fermi-Dirac integral of 3/2 order and Fermi-Dirac integral of 1/2 order is adopted to remove the derivates of Fermi-Dirac integral in the process of analyzing carrier heating effects in SOAs. The method allows us to use the global approximations of Fermi Dirac integral of 3/2 order and 1/2 order to obtain the analytical expression for carrier heating effects. Based on the energy band structure of SOAs, the non-global approximation of Fermi-Dirac integral of 1/2 order is suggested to reduce the computing time.

In the next section, influences from carrier heating on picosecond pulse amplification are investigated. It is found that the gain coefficient decreases due to the carrier density reduction and the increase of the carrier temperature in the process of signal amplification. The gain coefficient without carrier heating effects is larger than that with carrier heating effects in the initial stage of the pulse amplification. This is explained that, as the temperature increases, the quasi-Fermi level in the conduction band decreases and the quasi-Fermi level in the valence band increases. Due to the quick decrease of the carrier density, the gain coefficient without carrier heating effects is smaller in the later stage. Furthermore, the responses of input signals having different peak powers are simulated. It is found that carrier heating effects lead to the smaller peak power value of the output amplified signal and larger peak temporal shift of the output amplified signal. When the peak power value of the input pulse is higher, carrier heating effects impose a more significant distortion of the amplified output signal. Either enlarging the input signal power or increasing the pump current can enhance the effects of carrier heating in SOAs.

References

[1] Dailey, J.M., Koch, T.L.: Impact of carrier heating on SOA transmission dynamics for wavelength conversion. *IEEE Photon. Technol. Lett.*, **19**, 1078 (2007)

[2] Nambu, Y. and Tomita, A.:Spectral hole-burning and carrier heating effects on the transient optical nonlinearity of highly carrier-injected semiconductor. IEEE J. Quantum Electron., **30**, 1981(1994).

[3] Hall, K. L., Lenz, G. , Darwish, A. M. and Ippen, E. P.: Subpicosecond gain and index nonlinearities in InGaAsP diode lasers. Opt. Commun., **111**, 589(1994).

[4] Uskov, A.V. , Meuer, C., Schmeckebier, H., Bimberg, D.: Auger Capture Induced Carrier Heating in Quantum Dot Lasers and Amplifiers. Appl. Phys. Express ,**4**, 022202(2011)

[5] Occhi, L. , Ito, Y. , Kawaguchi, H. , Schares, L. , Eckner, J. , Guekos, G. : Intraband gain dynamics in bulk semiconductor optical amplifiers: measurements and simulations. IEEE J.Quantum Electron**. 38**, 54(2000).

[6] Gomatam, B. N. , DeFonzo, A. P. : Theory of hot carriers effects on nonlinear gain in GaAs/GaAlAs lasers and amplifiers. *IEEE J. Quantum Electron.,* **26**, 1689(1990).

[7] Tolstikhin, V. , Willander, M. , : Carrier heating effects in dynamic single-frequency GaInAsP–InP laser diodes. IEEE J. Quantum Electron., **31**, 814(1995).

[8] Mecozzi, A. , Mørk, J. ,:Saturation induced by picosecond pulses in semiconductor optical amplifiers. J. Opt. Soc.Am. B **14**, 761(1997)

[9] Hussain,K., Datta,P.K.: Effect of including intraband phenomena in the semiconductor optical amplifier model for propagation of short pulses. Applied Optics, **52**, 7171(2013)
[10] Uskov, A. V., Karin, J. R. , Bowers, J. E., McInerney, J. G., Bihan, J. L., :Effects of carrier cooling and carrier heating in saturation dynamics and pulse propagation through bulk semiconductor absorbers: IEEE J. Quantum Electron., **34**, 2162(1998).
[11] Blakemore, J. S. ,:Semiconductors Statistics. Pergamon, New York (1962) Appendices B and C.
[12] Blakemore, J. S. :Approximations for Fermi-Dirac integrals, especially the function $f_{1/2}(\eta)$ used to describe elctron density in a semiconductor. Solid-State Electronics, **2**,1067(1982)
[13] Coldren, L. A. , Corzine, S. W., Diode Lasers and Photonic Integrated Circuits. New York: Wiley, 1995.
[14] Dailey, J., Koch, T.: Simple rules for optimizing asymmetries in SOA-based Mach-Zehnder wavelength converters. Lightw. Technol., **27**, 1480(2009).
[15] Qin, C., Huang, X., Zhang, X.: Gain recovery acceleration by enhancing differential gain in quantum well semiconductor optical amplifiers. IEEE. Quantum Electron., **47**, 1443(2011).
[16] Aymerich-Humet. F, X. , Mestres, S., Millan, J.: An analytical approximation for the Fermi-Dirac integral $F_{3/2}(\eta)$. Solid-State Electronics, **24**, 981(1981)
[17] Nilsson, N. G. :Empirical approximations for the Fermi energy of a semiconductor with parabolic bands. Appl. Phys. Lett., **33**, 653(1978).
[18] Bednarczyk, D. , Bednarczyk, J. : The approximation of the Fermi-Dirac integral $F_{1/2}(\eta)$. Phys. Lett., **64A**, 409(1978).
[19] Chao, C. Y.-P., Chuang, S. L. : Spin-orbit-coupling effects on the valence-band structure of strained semiconductor quantum wells. Phys. Rev. B, **46**, 4110 (1992).
[20] Yariv, A. , Opt. Electron. , HWR International, New York, 1985.
[21] Connelly, M. J. :Wideband semiconductor optical amplifier steady-state numerical model. IEEE J. Quantum Electron., **37**, 439(2001).
[22] Adachi, S.,GaAs and related materials, World Scientific,Singapore,1994
[23] Chuang, S. L. , Physics of Optoelectronic Devices. New York: Wiley, 1995.
[24] Ghafouri-Shiraz, H. , Tan, P. W. :Study of a novel laser diode amplifier structure. *Semicond. Sci. Technol.,* **11** ,1443 (1996).